Romanian Reports in Physics, Vol. 62, No. 2, P. 329–340, 2010

HYDROGEN-PLASMA INDUCED PLATELETS AND VOIDS IN SILICON WAFERS

C. GHICA[1, *], L.C. NISTOR[1], B. MIRONOV[1], S. VIZIREANU[2]

[1]*National Institute of Materials Physics, Str. Atomistilor Nr. 105 bis, 077125 Bucharest-Magurele, Romania*
[2]*National Institute for Laser, Plasma and Radiation Physics, Str. Atomistilor Nr. 409, 077125 Bucharest-Magurele, Romania*

(Received August 4, 2009)

*Abstract. S*ilicon wafers have been submitted to hydrogen RF-plasma treatment in various experimental conditions. The hydrogen RF-plasma treatment on Si wafers induces two kinds of effects: surface corrugation and formation of structural defects below the wafer surface. The structural defects resulted after the plasma treatments have been investigated by conventional and high-resolution transmission electron microscopy (CTEM and HRTEM) techniques. The specificity of the induced extended defects due to hydrogen decoration has been emphasized.

Key words: plasma treatment, extended defects, transmission electron microscopy.

1. INTRODUCTION

In materials science, mastering structural defects down to atomic level represents a key aspect in the effort of developing new materials or tailoring the physical and chemical properties of present materials. This paper deals with structural defects induced in silicon wafers, aiming at modifying their mechanical properties in an extremely thin surface layer. The defects are induced via hydrogen plasma treatment in various experimental conditions. Hydrogen induced defects in silicon have been intensively studied concerning the doping control and defect passivation. Changing its mechanical properties by controlled defect creation is of great interest in the SOI (silicon on insulator) device fabrication based on the "smart-cut" technique [1]. The "smart-cut" method involves the exfoliation of a crystalline silicon layer, followed by attaching it to a desired substrate (e.g. amorphous insulating substrate). This could be achieved by creating a high density of defects at a certain depth under the wafer surface. Ion implantation of light atoms such as H or He is nowadays used to create crystal defects with a certain distribution profile under the Si wafer surface [2]. Silicon treatment in hydrogen plasma is considered as an alternative softer way in creating subsurface defects in a

layer even thinner than the one obtainable by ion implantation [3-8]. Before any technological approach, it is of maximum importance to find out the structural effects of the hydrogen plasma treatment on silicon, to identify and characterize by appropriate techniques the induced defects. The main effect of the hydrogen plasma treatment on the Si wafers is the formation of defects referred to as H-platelets [9, 10]. This paper contains microstructural results obtained by transmission electron microscopy intending to give a general view regarding the effects of the hydrogen RF-plasma treatment on silicon wafers and to determine the specificity of the hydrogenation-induced defects with respect to ordinary structural defects in Si.

2. EXPERIMENTAL

We have applied hydrogen RF-plasma treatments (13.56 MHz RF generator) on silicon wafers varying the hydrogen partial pressure in the $10\text{-}10^4$ Pa range and the discharge power between 50-150 W. The sample temperature during the interaction with the RF-plasma did not exceed 200 ^{o}C. The treatment duration was varied from 1 h to 4 h. The as-treated samples have been investigated by conventional and high-resolution transmission electron microscopy (CTEM/HRTEM) using the JEOL 200 CX and JEOL 4000 EX microscopes. The TEM specimens have been prepared in plan-view and cross-section by mechanical thinning and ion milling on a Gatan PIPS machine.

3. RESULTS AND DISCUSSIONS

For the identification and characterization of the induced defects, we have first used CTEM techniques, where extremely valuable information can be extracted by analyzing the diffraction contrast of the defects for various specimen orientations. For further in-depth analysis of the identified defects, we have carried out HRTEM investigations on our samples.

3.1. CTEM RESULTS

Morphological and structural information about the effects induced by hydrogen plasma irradiation in silicon wafers were obtained by CTEM investigations on cross-section specimens (Fig. 1). There are two effects of the hydrogen RF-plasma treatment on Si wafers: a surface effect consisting in a surface corrugation and a subsurface effect consisting in the formation of structural defects. The amplitude of these effects is determined by the treatment conditions, such as the treatment duration or the power of the RF discharge.

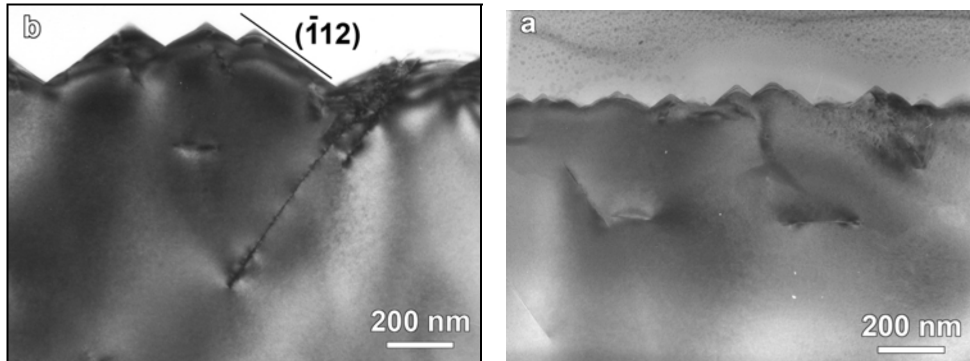

Fig. 1 – Surface roughness and extended structural defects the below surface in the case of a Si(100) wafer treated in hydrogen RF-plasma during 1 h (a) and 4 h (b).

The surface roughening is caused by a non-homogeneous etching of the Si wafer in the hydrogen plasma, leading to the formation of micropyramids with {112} crystallographic planes as lateral faces. The importance of the treatment duration results from comparing the surface roughness in the case of Si(100) wafer treated in the hydrogen RF-plasma for 2 h and 4 h. The sample treated for 2 h shows a surface roughness with peak-to-peak level variations around 100 nm and a high density of defects right under the surface. The surface roughness in the case of the 4 h treated sample is significantly increased, reaching peak-to-peak level variations up to 300 nm. The density of structural defects in the proximity of the free surface decreases with respect to the 2 h treated sample, due to the etching effect competing to the formation of subsurface defects. However, in both cases, large defects can be noticed running deep under the surface of the treated samples, intercepting or not the free surface of the sample. Surface corrugation is an undesirable effect for microelectronics applications, which is the reason why the experimental conditions need to be optimized in order to reduce or eliminate the surface effects.

The second effect of the hydrogen plasma treatment is the formation of structural defects under the surface of the treated wafer, which is the most important aspect of the hydrogenation treatment, concerning its further application to the “smart-cut” technique. Like for the surface corrugation, the treatment conditions play an essential role in the formation of these defects. Their size, density and depth under the free surface of the wafer are highly dependent on the RF-plasma parameters and treatment duration.

Planar defects having {111} as habit planes are usual for materials with cubic structure, including materials with cubic diamond structure, such as silicon. The typical example of a planar defect in materials with cubic diamond structure is the stacking fault resulting from the dissociation of a perfect dislocation into partials. The slip system in silicon is <110>{111}, in which dislocations lie along the

<110> directions with the possibility to slip across the dense {111} planes. However, as we will show hereafter, the {111} defects in the hydrogenated Si wafers have features which distinguish them from the regular {111} defects in materials with diamond structure.

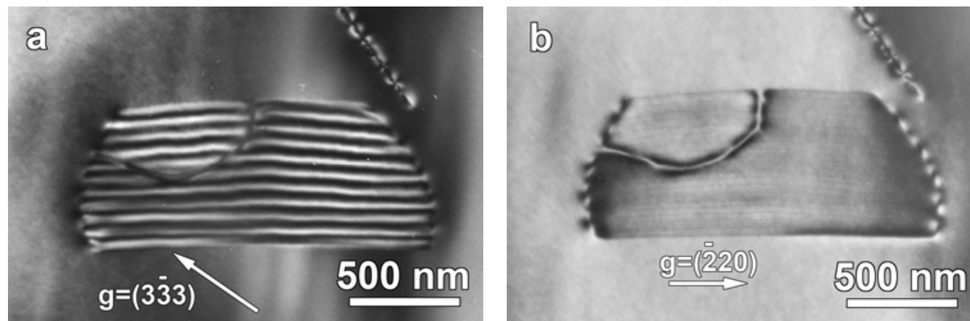

Fig. 2 – Bright-field TEM image (a) of a {111} planar defect with the $3\bar{3}3$ reflection strongly excited; (b) bright-field TEM image showing fringe extinction when the $\bar{2}20$ reflection is strongly excited.

Fig. 2 shows typical diffraction contrast images of the {111} defects found in many of our plasma hydrogenated Si samples. When cross-section specimens are cut perpendicular to the [110] zone axis, these defects are observable either as edge-on or as bright/dark fringes parallel to the wafer free surface. Typically, the characteristic fringes are not straight, but slightly curved or undulated, indicating that the defect is not limited to a single crystallographic plane, but it "migrates" to adjacent planes. In a previous publication [11] we have demonstrated from the diffraction contrast behavior that the defects have an intrinsic character (missing silicon plane) [12]. The characteristic fringes of the defect become invisible for $\mathbf{g} = (2\bar{2}0)$, showing that the characteristic displacement vector **R** has no components along $[2\bar{2}0]$ and it is most probably oriented perpendicular to the habit plane, as in the case of regular stacking faults [12].

The second type of defects introduced by RF-plasma hydrogenation in silicon are the planar defects oriented along {100} planes. The {100} planar defects are not encountered in diamond cubic materials, as {100} is not a slip plane in these crystallographic systems. However, {100} platelets have been reported for Si and Ge wafers submitted to deuteron irradiation [9, 13]. The diffraction contrast of the {100} planar defects in hydrogenated Si is presented in Fig. 3 for two different orientations, with the $2\bar{2}0$ and $00\bar{4}$ reflections excited. Two planar defects bordered by dislocation loops can be noticed. The fringes inside the dislocation loop indicate the presence of a planar defect. In the two-beams situation with the $00\bar{4}$ reflection excited, the inner vertical fringes become invisible. The extinction of the internal fringes indicates that the characteristic displacement vector **R** is oriented perpendicular to the $(00\bar{4})$ reciprocal vector, thus belonging to the (001)

plane. We have shown [14] that the limiting dislocation loops have a prismatic character, with the Burgers vector of the dislocation out of the loop plane. However, due to the unusual crystalline nature of the planar defect inside the dislocation loop, the determination of a precise value for the Burgers vector is not obvious. Using the invisibility criterion we came to the conclusion that the Burgers vector is situated in the (001) plane, most likely either 1/2 $[\bar{1}10]$ or 1/2 $[1\bar{1}0]$. The fact that the dislocation loops limit defected areas showing bright/dark fringes suggests that the Burgers vector might be of the 1/y[110] kind, with y≈2, as suggested by the {111}[110] slip system in diamond cubic structures and verified by the invisibility criterion.

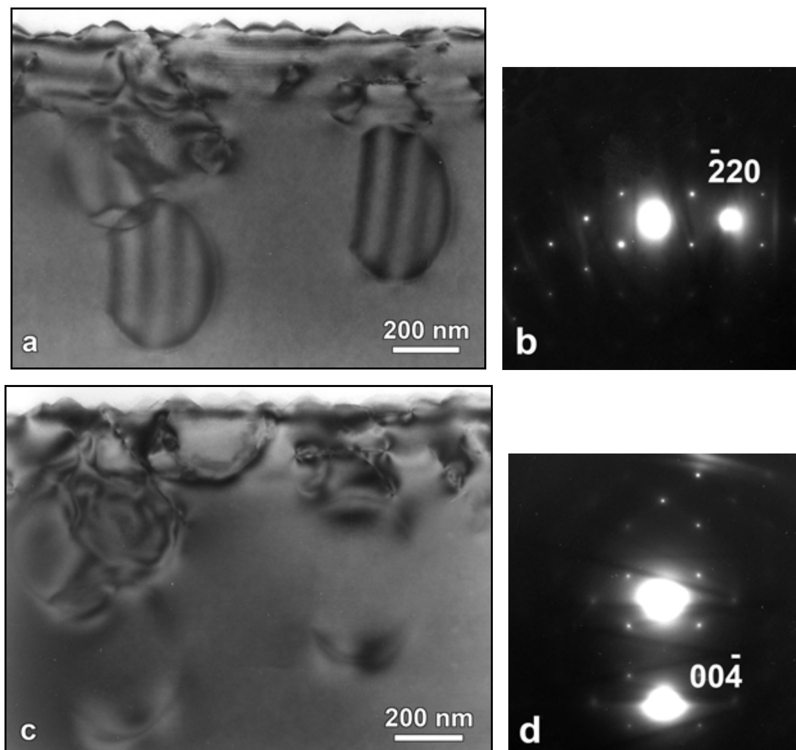

Fig. 3 – Bright-field TEM images of the (100) planar defects limited by dislocation loops in two-beams conditions: $2\bar{2}0$ reflection strongly excited (a, b) and $00\bar{4}$ reflection excited (c, d). The specimen orientation is close to **B** = [110]. Notice the fringe extinction in the case of the $00\bar{4}$ strong reflection.

The third type of the observed extended defects consists in nanometric voids in the hydrogenated Si wafers. From previous observations on He implanted silicon [3], we expected to observe bubbles in hydrogenated Si, as well. However, TEM observations revealed their rather seldom presence both in plan-view and cross-section specimens. In general, they appear as agglomerations of bubbles around

5–20 nm in size and they are surrounded by long-range strain field; when imaged in plan-view close to the [001] zone axis, a 4-fold symmetry contrast surrounds them (Fig. 4). In order to elucidate the origin of this contrast, we have performed tilting and defocus variation experiments.

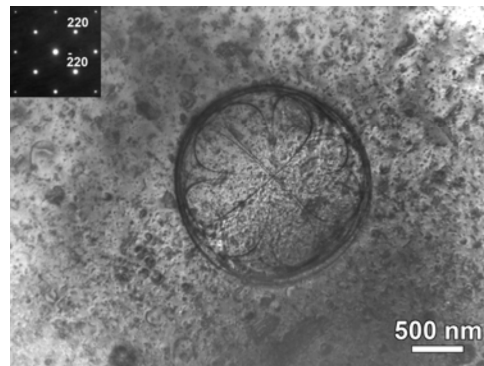

Fig. 4 – 4-fold symmetric strain field noticed in plan-view specimens of hydrogenated Si wafers.

Fig. 5 shows two-beams images of the defect, **g** = $(0\bar{4}0)$, in a plan-view specimen prepared from a hydrogenated Si(001) wafer. The two images present a bubble agglomeration surrounded by an asymmetrical 2-lobed strain field contour. The nature of the defect can be resolved on the over focused ($\Delta f > 0$) and under focused ($\Delta f < 0$) images. For negative defocus the bubbles show a bright inner fringe, while for positive defocus the inner fringe becomes dark, which is the typical contrast behavior for cavities inside a solid matrix [15].

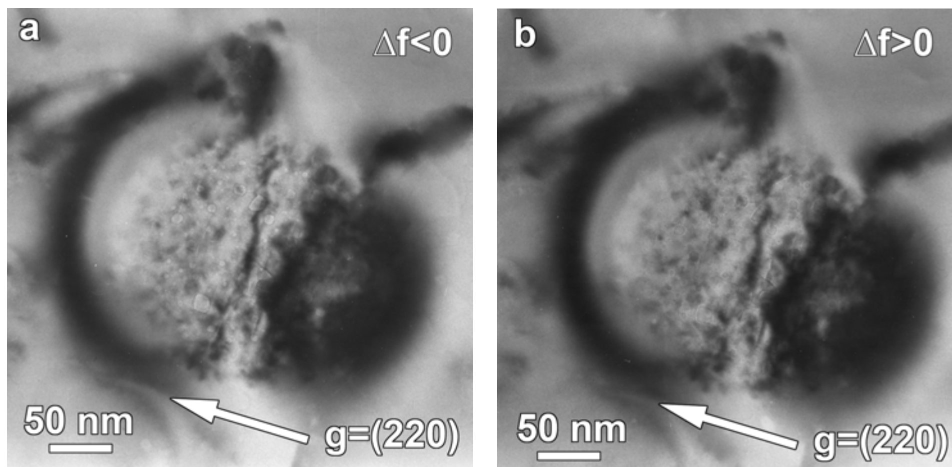

Fig. 5 – Identification of nanometric voids in hydrogenated Si evidenced by objective-lens focus variation: negative defocus in (a) and positive defocus in (b).

The location of the created nanometric cavities with respect to the wafer fee surface is very important regarding the “smart-cut” procedure. However, due to their low density, it is very difficult to image them on cross-section specimens. We present in Fig. 6 the cross-section TEM image of such a cavity in RF-plasma hydrogenated Si. The nanometric cavity is rather large (almost 100 nm) and is situated deep under the surface at about 500 nm. As noticed on the plan-view images, the cavity is accompanied by a long-range strain-field revealed by the concentric dark diffraction contours.

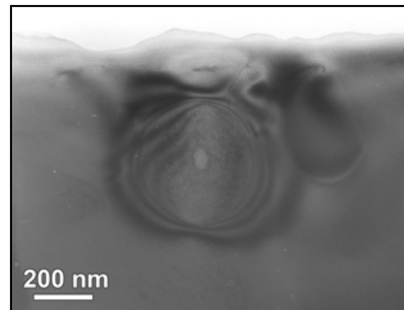

Fig. 6 – Cross-section TEM image showing a nanometric (<100 nm) cavity and the long-range surrounding strain field deep (~ 500 nm) under the free surface of a hydrogenated Si wafer.

3.2. HRTEM OBSERVATIONS

Most of the {111} defects observed in our specimens intercept the free surface of the hydrogenated wafer. The HRTEM contrast at the defect emergence location (Fig. 7a) reveals a funnel-like surface opening continuing below the surface with a planar defect in a {111} habit plane. In the thinnest areas of the specimen, the defect appears as one row of brighter spots (depending on the defocus).

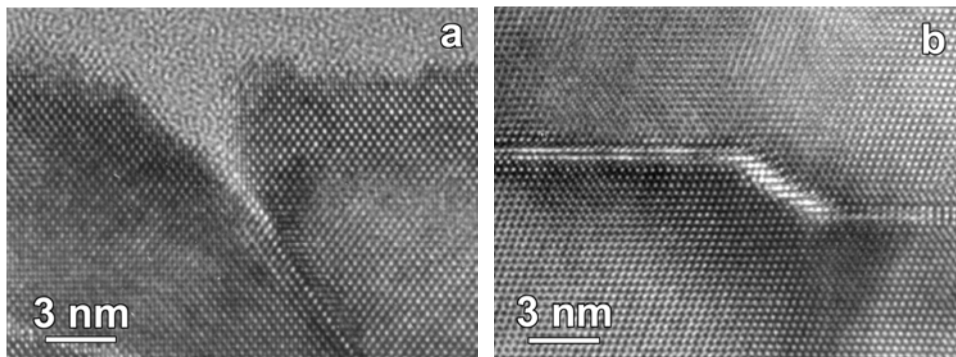

Fig. 7 – HRTEM images of {111} planar defects in hydrogenated Si: a) defect intercepting the free surface of the wafer in a thin area of the specimen; b) step along a {111} defect showing the defect migration across several {111} planes.

In the thicker regions of the specimen the {111} defects exhibit various HR patterns in precise [110] zone axis orientation, most frequently like two rows of brighter spots along the {111} planes concerned. The interpretation of the HRTEM image of the {111} defects is not obvious. This is due to the high strain field around the {111} defects in hydrogenated Si, which can be noticed even at low magnifications by diffraction contrast. The high strain field could be related to the presence of hydrogen decorating these defects. The strain distribution along the defect is not homogeneous, as one can see for the edge-on defects. The presence of the high strain field strongly alters the HRTEM contrast along the defect. A variation and even inversion of the phase contrast across the defect can be observed. Moreover, the defect is not strictly limited to a single {111} plane, but it migrates to adjacent {111} planes forming jogs (Fig. 7 b). This fact explains the curvature and deformations of the fringes on the diffraction contrast images of the {111} defects. We have previously made a detailed analysis of the {111} defects in hydrogenated silicon by quantitative characterization of the strain field around the defect and we have suggested a structural model able to reproduce the experimental HRTEM pattern observed in our micrographs [11]. The structural model that we proposed for the {111} defects in hydrogenated silicon involved Si dangling bonds that could be partially saturated with hydrogen. Therefore, the {111} planar defect could be described as a collection of H_2* defects [16, 17] lined up on a {111} plane.

The HRTEM images of edge-on {100} defects in hydrogenated Si wafers are also difficult to analyze due to the presence of a high strain field around these defects. Moreover, unlike the {111} defects, the {001} defects are rather unstable in the electron beam and special precautions are necessary when recording HR images. It is well known that for accelerating voltages higher than 300 kV, the electron beam creates defects in Si by a knock-on mechanism.

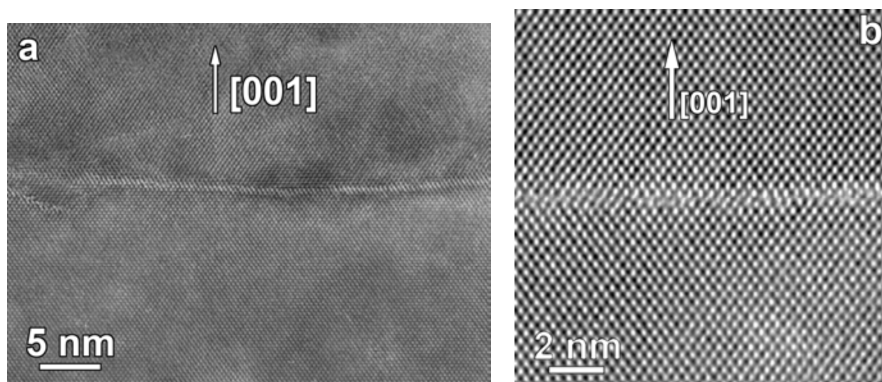

Fig. 8 – a) Cross-section HRTEM image of a curved (001) planar defect in hydrogenated Si. b) detailed HRTEM image of a (001) defect in hydrogenated Si.

We noticed this effect in our specimens during the observation in HR conditions at 400 kV. However, while the {111} defects were not beam sensitive, the {001} defects disappeared after about 20 seconds of observation in HR conditions at 400 kV. A low-magnification image of an edge-on (001) defect in RF-plasma hydrogenated Si is presented in Fig. 8a. Like the {111} defects, it migrates to adjacent planes, which gives it a slightly curved lens-like shape. A fragment from the central region of such a defect in edge-on orientation is imaged in Fig. 8b. The defect is not limited to a single crystallographic plane. It has a diffuse aspect affecting two or three neighboring (001) planes. The loss of fringe contrast can be related to a high degree of disorder in the lattice. By Fourier filtering of the HR images we have shown [14] that the HR fringes show important distortions along the defect, where fragments of interstitial (002) planes can be observed. Therefore, the defect has not a unique extrinsic or intrinsic character, but rather a mixed one.

3.3. DISCUSSION

A discussion on the formation mechanism of these defects in hydrogenated Si should have in view two aspects regarding the interaction between the hydrogen plasma and the Si wafers. In the first place, due to their small size, hydrogen atoms can easily diffuse through the Si lattice. Secondly, it is well known that hydrogen ions in RF-plasma are extremely active with respect to the covalent bonds in Si, which explains the high corrosive effect on the Si wafers. Therefore, there are two processes occurring in the same time: i) surface etching by inhomogeneous material removal and formation of faceted pyramidal humps on the surface; ii) formation of defects below the surface. These defects might be grouped in two categories depending on their position with respect to the treated surface: surface defects, created in the first 50 nm below the surface and/or intercepting the wafer surface, and buried defects, appearing deep under the wafer surface, up to several hundreds of nanometers or even microns. Most of the induced defects are surface defects, appearing in the close vicinity of the free surface. The surface defects are in competition with the etching effect, which explains why samples treated during 4 h show a high roughness but a relatively low density of surface neighboring defects.

The {111} defects in plasma-hydrogenated silicon have an intrinsic character (missing Si plane) [11, 12], as demonstrated both by diffraction contrast and quantitative HRTEM analysis. Most of the {111} defects intercept the hydrogen treated surface. Judging by the funnel-like aspect of the defect at the intersection with the wafer surface, we believe that they are formed through a mechanism involving silicon etching and hydrogen diffusion into the Si lattice. Si atoms are

removed from the structure as a result of the etching effect of the H-plasma on the Si wafer, followed by a partial saturation of the resulting dangling bonds with H atoms diffused in the silicon matrix.

The {001} platelets do not communicate with the wafer surface (in the case of Si(001) wafers) and they might appear even deeper under the surface. They are surrounded by dislocation loops, resulting probably from the accumulation of vacancies and self-interstitials followed by their condensation on a {001} plane. It is well known in literature that this mechanism represents the way in which prismatic dislocation loops are formed [18]. Since this kind of defect is not characteristic to silicon, but it occurs only in hydrogenated wafers, one could infer that the vacancies and interstitials involved are generated from the interaction between the Si lattice and the in-diffused H atoms.

In the case of the observed lattice voids, the formation mechanism seems to be the same as in the case of the {001} defects, namely an accumulation of in-excess vacancies. The interaction between the in-diffused H atoms and the Si lattice, based on the high chemical reactivity of the H atoms against the Si-Si bonds, is at the origin of the lattice vacancies and self-interstitials formation. These agglomerations of nano-cavities are always surrounded by long-range strain-field contours, demonstrating that high mechanical tensions are concentrated here. It is difficult to say, based only on the presence of the long-range strain filed, whether the observed nanometric cavities contain or not gaseous hydrogen. However, previous Raman measurements on similar samples [19] revealed the presence of molecular hydrogen which might be associated with the existence of such nanometric cavities in hydrogenated silicon.

4. CONCLUSIONS

Hydrogen RF-plasma treatment induces two kinds of effects on Si wafers, depending on the treatment conditions: surface corrugation and formation of structural defects under the wafer surface. The created defects show characteristic features attributable to the hydrogen presence. They are all surrounded by a long range strain field, which complicates the HRTEM investigation. The samples contain {001} planar defects which are unusual for materials having the diamond cubic structure. These defects are not limited to a single crystallographic {001} plane, but they affect several neighboring planes. The {001} defects are limited by prismatic dislocation loops with a Burger vector of the $1/y[110]$ kind, with $y \approx 2$. They have a mixed extrinsic and intrinsic character, appearing most seemingly by accumulation of in-excess vacancies and self-interstitials. The {111} defects have an intrinsic character (missing Si plane), but because they are decorated with

hydrogen, they differ from regular {111} defects in Si, as shown by the TEM/HRTEM images. Agglomerated nanometric cavities accompanied by a long-range strain field have also been noticed in our samples. These nanocavities might contain hydrogen in molecular state, as deduced by other authors using Raman investigations.

Acknowledgement. This work has been financially supported by CNCSIS in the frame of the PN II Ideas national research program (Project No. 233/2007).

REFERENCES

1. M. Bruel, *Application of hydrogen ion beams to Silicon On Insulator material technology*, Nucl. Instrum. Meth., B, **108**, 313–319 (1996).
2. M.F. Beaufort, H. Garem, J. Lepinoux, *Microstructural defects induced by implantation of hydrogen in (111) silicon*, Philos. Mag., **A 69**, 881–901 (1994).
3. G.F. Cerofolini, F. Corni, S. Frabboni, C. Nobili, G. Ottaviani, R. Tonini, *Hydrogen and helium bubbles in silicon*, Mat. Sci. Eng., **27**, 1–52 (2000).
4. N.H. Nickel, G.B. Anderson, N.M. Johnson, J. Walker, *Nucleation of hydrogen-induced platelets in silicon*, Phys. Rev., **B 62**, 8012–8015 (2000).
5. H. Nordmark, R. Holmestad, J.C. Walmsley, A Ulyashin, *Transmission electron microscopy study of hydrogen defect formation at extended defects in hydrogen plasma treated multicrystalline silicon*, J. Appl. Phys., **105**, 033506 (2009).
6. P.F.P. Fichtner, J.R. Kaschny, M. Behar, R.A. Yankov, A. Mücklich, W. SkorupA, *The effects of the annealing temperature on the formation of helium-filled structures in silicon*, Nucl. Instrum. Meth., **B 148**, 329–333 (1999).
7. C. Qian, B. Terreault, S.C. Gujrathi, *Layer splitting in Si by H+He ion co-implantation: channeling effect limitation at low energy*, Nucl. Instrum. Meth., **B 175-177**, 711–714 (2001).
8. S. Rangan, S. Ashok, G. Chen, D. Theodore, *Multi-layered nanocavities in silicon with sequential helium implantation/anneal*, Nucl. Instrum. Meth., **B 206**, 417–421 (2003).
9. S. Muto, S. Takeda, *New stable defect structure on the {001} plane in germanium formed by deuteron irradiation*, Phil. Mag. Lett., **72**, 99–104 (1995).
10. N.M. Johnson, F.A. Ponce, R.A. Street, R.J. Nemanich, *Defects in single-crystal silicon induced by hydrogenation*, Phys. Rev., **B 35**, 4166–4169 (1987).
11. C. Ghica, L.C. Nistor, H. Bender, O. Richard, G. Van Tendeloo, A. Ulyashin, *Characterization of {111} planar defects induced in silicon by hydrogen plasma treatments*, Philos. Mag., **86**, 5137–5151 (2006).
12. P.B. Hirsch, A. Howie, R.B. Nicholson, D.W. Pashley, M.J. Whelan, *Electron Microscopy of Thin Crystals,* Butterworth & Co., London, 1967, p. 165.
13. T. Akatsu, K.K. Bourdelle, C. Richtarch, B. Faure, F. Letertre, *Study of extended-defect formation in Ge and Si after H ion implantation*, Appl. Phys. Lett., **86**, 181910 (2005).
14. C. Ghica, L.C. Nistor, H. Bender, O. Richard, G. Van Tendeloo, A. Ulyashin, *TEM characterization of extended defects induced in Si wafers by H plasma treatment*, J. Phys. D: Appl. Phys., **40**, 395–400 (2007).
15. D. Williams, C.B. Carter, *Transmission Electron Microscopy*, Vol. 3, Plenum, New York and London, 1996, p. 451.

16. M.K. Weldon, V.E. Marsico, Y.J. Chabal, A. Agarwal, D.J. Eaglesham, J. Sapjeta, W.L. Brown, D.C. Jacobson, Y. Caudano, S.B. Christman, E.E. Chaman, *On the mechanism of the hydrogen-induced exfoliation of silicon*, J. Vac. Sci. Technol., **B 15**, 1065–1073 (1997).
17. E.V. Lavrov, J. Weber, *Structural properties of hydrogen-induced platelets in silicon: a Raman scattering study*, Physica, **B 308-310**, 151–154 (2001).
18. D. Hull, *Introduction to Dislocations*, 2nd edition, Pergamon, Oxford, 1975, p.76.
19. A.G. Ulyashin, R. Job, W.R. Fahrner, O. Richard, H. Bender, C. Claeys, E. Simoen, D. Grambole, *Substrate orientation, doping and plasma frequency dependencies of structural defects formation in hydrogen plasma treated silicon*, J. Phys. – Condens. Mat., **14**, 13037–13045 (2002).